RSC Advances

PAPER

View Article Online
View Journal | View Issue

Cite this: *RSC Adv.*, 2023, **13**, 30915

Molecular insights into the interfacial adhesion mechanism between carbon nanotubes and epoxy resin

Songyue Chai, Jiao Liu, Dongshuai Hou and Pan Wang*

Received 23rd August 2023
Accepted 14th October 2023

DOI: 10.1039/d3ra05749f

rsc.li/rsc-advances

In recent years, carbon nanotubes (CNTs) have garnered widespread attention and have been deemed the preferred option for the creation of epoxy composites, owing to their outstanding mechanical properties. Despite this, the interaction between pure CNTs and epoxy resin is primarily dependent on van der Waals forces and therefore, the interfacial forces are weak, making it challenging for effective load transfer. To enhance the mechanical properties of the composites, surface functionalization is often deemed a more favorable method for improving interfacial bond strength. This study employs molecular dynamics simulations to examine the interfacial bonding characteristics between functionalized CNTs and epoxy resin. The results demonstrate that functional group modification can significantly improve the interfacial adhesion between CNTs and epoxy resin, and the incorporation of functional groups can enhance the crosslinking degree of the epoxy resin at the interface. The hydrogen bond network established between the CNTs and epoxy resin after functional group modification, and the high stability of the bond cooperation, are factors contributing to the excellent interfacial performance.

1 Introduction

Epoxy resin is a three-dimensional crosslinked thermosetting material composed of a bisphenol-A epoxy resin monomer and a suitable curing agent, characterized by its excellent stability, heat resistance, favorable chemical corrosion resistance, and electrical insulation.[1–3] The material has seen widespread applications in industries such as aerospace, building materials, and electronic communications. However, despite its high crosslinking density, epoxy resin is known for its low absolute strength, poor fracture toughness, and high brittleness, leading to weak impact resistance and limited lifetime and application range of the composites.[4,5] Therefore, it becomes imperative to investigate methods to improve the mechanical performance of epoxy resin.

The advancement of nanotechnology has presented a new approach to enhance the mechanical properties of polymer systems. Numerous studies have demonstrated that the mechanical performance of epoxy resin can be improved through the doping of nanoparticles, such as TiO_2,[6–8] silica,[9,10] and carbon nanotubes.[11,12] Carbon nanotubes (CNTs) have garnered extensive interest due to their unique physical and chemical properties[13] since Iijima *et al.*[14] published the first article on them in 1991. CNTs are typical one-dimensional nanoparticles with a high specific surface area and light weight,[15,16] and possess excellent tensile strength along their longitudinal axis.[17,18] Utilizing CNTs as nanomaterials to improve the mechanical properties of composites has garnered interest in both experimental and theoretical studies.[19–21] Experimental studies have demonstrated that incorporating CNTs into epoxy resins has a positive impact on the mechanical properties of composites, such as the elastic modulus and tensile strength. For instance, Chen *et al.*[22] found that grafted polymers on CNTs improved the compatibility between CNTs and epoxy resins, leading to strong interfacial chemical bonding, and a 68% increase in tensile strength was achieved through the modification of epoxy resins with CNTs after grafting, attributed to the formation of a CNT network that transfers part of the external load. Bansal *et al.*[12] suggested that uniform dispersion of CNTs within the polymer, even in small amounts, can result in a significant improvement in the mechanical properties of epoxy composites. This conclusion provides a valuable direction for the advancement of the field of CNT composites. The high interfacial area and bridging mechanism properties of MWCNTs are effective in suppressing the growth of nano-pores and inhibiting crack propagation in the substrate, thus enhancing the properties of the composites.[23] In addition to the above experimental studies, molecular dynamics (MD) techniques are widely utilized across various fields, including polymer composites. A comprehensive systematic investigation of nanoparticle-reinforced epoxy resins has been conducted. Hou *et al.*[24] employed atomic simulations to examine the mechanism behind the impact of graphene oxide on the bonding mechanism at the interface between epoxy resin and calcium silicate hydrate (CSH). They proposed

Department of Civil Engineering, Qingdao University of Technology, Qingdao 266033, China. E-mail: wangpan@qut.edu.cn

that strong interfacial bonding cooperation is the key factor responsible for the enhanced bonding effect. Sul *et al.*[25] performed simulations of carbon nanotubes (CNTs) in epoxy resin and suggested that CNTs can increase the elastic modulus of composites and decrease the glass transition temperature. The poor solubility of nanomaterials in polymers can result in inadequate mechanical properties of composites.

However, it should be noted that extensive research has demonstrated a significant relationship between the performance of epoxy resin composite materials and the interfacial bonding ability of epoxy resin, regardless of the type of nanomaterial incorporated. Baudot *et al.*[26] found that incorporating carbon nanotubes into the epoxy resin matrix during the polymerization process leads to improved mechanical strength and enhanced heat transfer. Hou *et al.*[27] discovered that the mechanical properties of epoxy resin modified with graphene oxide (GO) depend on the bonding strength between GO and epoxy resin. Wang *et al.*[28] suggested that the interfacial strength and adsorption capacity of epoxy resin significantly affect the strength of concrete structures. Mao *et al.*[29] also observed that the bonding interaction between carbon nanotubes and the epoxy resin matrix effectively enhances the properties of the nanocomposites.

Therefore, enhancing the interfacial adhesion between the polymer and carbon nanotubes will greatly improve the performance of epoxy resin composite materials. To address the aforementioned challenges, covalent functionalization of carbon nanotubes has been identified as a viable solution for improving the interfacial interactions.[30–33] Wang *et al.*[34] employed the grafting of polymers onto multi-walled carbon nanotubes as a means to toughen epoxy composites, and the results revealed that the modified nanotubes resulted in uniform dispersion of CNTs, which were hindered from lateral interactions and led to enhanced interfacial bonding between CNTs and the epoxy resin. Ma *et al.*[35] conducted amination treatment on the surface of CNTs, and observed a significant improvement in the stability of CNTs. Jung *et al.*[36] verified through experiments and simulations that improving interfacial adhesion is crucial for enhancing the mechanical properties of polymer composites.

Nevertheless, most researchers have primarily focused on the impact of CNTs on the mechanical properties of composites, and only a few have briefly discussed the effect of functional groups. The mechanism behind the impact of functional groups on interfacial bonding remains unclear, impeding the progress of epoxy resin-reinforced materials.

Considering the strong correlation between mechanical properties of composites and interfacial adhesion, this paper investigates the effect of functional groups on the interfacial bonding mechanism of epoxy resin composites using molecular dynamics. Three composites reinforced with single wall CNTs, including unfunctionalized, hydroxyl-functionalized, and carboxy-functionalized groups, were established to observe differences in interfacial bonding properties through pull-out simulations of CNTs. This study is expected to offer a novel understanding of the principles of CNT-reinforced composites and provide a new perspective for the advancement of nano-reinforced composites.

2 Computational methods

2.1 Model construction

The two main components of a crosslinked epoxy are bisphenol A (DGEBA) as the monomer and isophorone diamine (IPD) as the crosslinker. The atomic structure of these components is depicted in Fig. 1(a). In this study, a 1 : 1 molar ratio of DGEBA and IPD were crosslinked to produce epoxy resin, resulting in a final crosslinking degree of 86%, satisfying the requirement for cross-linking determined by experimental studies (≥80%).[37,38] The cell density of the epoxy was maintained at 1.131 g cm^{-3}, which is in close agreement with the reported epoxy resin density values of 1.07–1.34 g cm^{-3} provided in the ref. 38 and 39. The crosslinking procedure was based on the methods proposed by Jian[40] and Jeyranpour.[41] The crosslinking process involved placing DGEBA and IPD in a predefined three-dimensional box. The reactive atom of DGEBA was designated as R1 and the reactive atom of IPD as R2. The reactive sites were identified within the reactive radius. For instance, the reactive carbon atom of DGEBA was selected, and then the reactive nitrogen atom of IPD was sought in proximity to the carbon atom. If R1 and R2 were within a specified reaction cutoff radius, covalent bonds between C–N atoms were formed, corresponding to the ring-opening of epoxy resin and the addition reaction of the curing agent. The cut-off radius range was set at 3.5–8 Å, with a 0.5 Å interval. The crosslinking temperature was maintained at 500 K, and the target crosslinking degree was 100%. Finally, the system was optimized over a short term to mitigate any adverse interactions resulting from bonding.

The atomic structure of single wall CNTs is illustrated in Fig. 1(b). The CNTs are constructed as follows: the CNT cell (x = 11.483 Å, y = 11.483 Å, z = 2.459 51 Å, $x = y = 90°$, $z = 120°$) is selected with $n = m = 6$ and a diameter of 8.14 Å. This cell is then expanded by 15 in the z direction to match the size of the epoxy resin. Hydroxyl (–OH) and carboxyl (–COOH) functional groups are then placed in the same position on the CNTs, with 16 functional groups in total. This placement of the functional groups at the same position helps to reduce the influence of positional differences.

The interface between carbon nanotubes (CNTs) modified with different functional groups and epoxy resin is simulated through the construction of three models: CNT/epoxy, CNT-OH/epoxy, and CNT-COOH/epoxy. As depicted in Fig. 1(c), the carbon nanotubes are centered within a box of dimensions 40 Å × 40 Å × 100 Å. To simulate the process of CNT failure at the crack location within the loaded epoxy resin matrix as shown in Fig. 1(c) due to pulling.

2.2 Computational details

The Consistent Valence Force Field (CVFF) is applied to model the interatomic potential between epoxy molecules and CNTs. This force field has been extensively used in the simulation of epoxy-CNT interface bonding, as evidenced by various

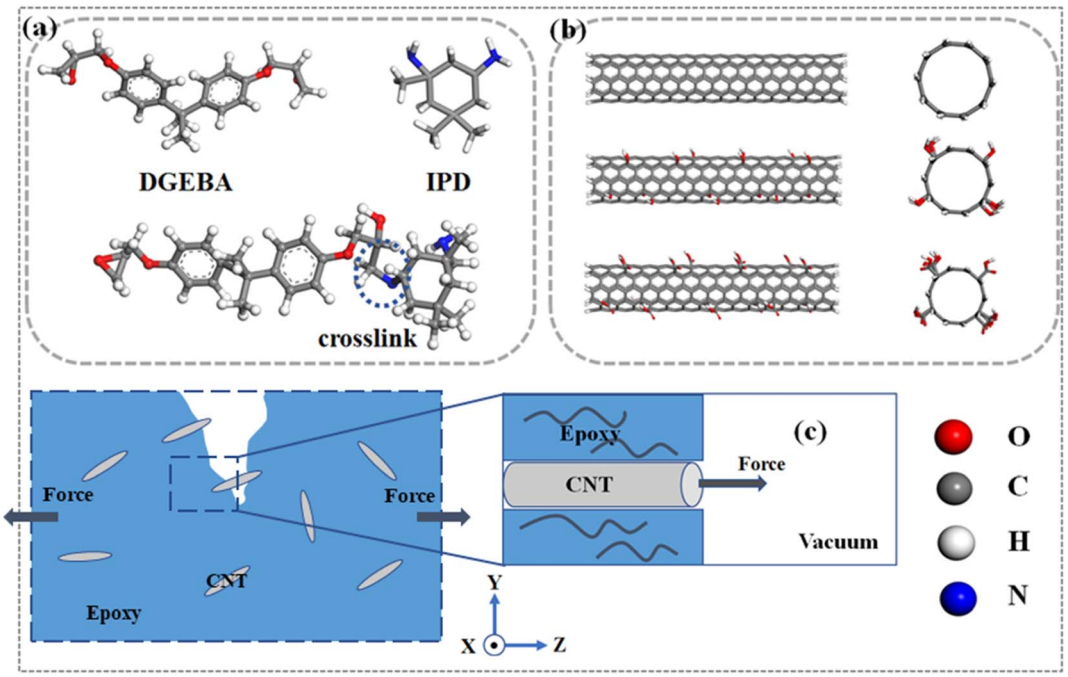

Fig. 1 (a) Epoxy molecule (b) functionalized carbon nanotubes (c) CNTs/epoxy interface model schematic diagram.

studies.[40–42] The MD simulations were performed using the LAMMPS software.[43] To obtain the global and local minimum energy configurations, eliminate irrational structures, and reduce internal stress, the initial structure underwent geometric optimization and dynamic relaxation. The calculation of the static structure was divided into two stages. The whole dynamics process was carried out using the NPT ensemble. In the first stage, the ambient temperature was set to 300 K and the time step was 1 fs. In the second stage, a dynamics simulation of 2 ns was performed, with a collection interval of 1 ps for the atomic trajectories. 2000 atomic trajectories were obtained to analyze the microstructure and dynamic properties of CNTs/epoxy composites. In the dynamic simulation process, the first two stages of the pull-out process were identical. In the third stage, the external force applied to the carbon nanotube during the pull-out process was extracted, and a force-displacement curve was generated. The pull-out force acted on the hydrogen atom closest to the vacuum layer, and the external force was calculated using the following formula:

$$F_{\text{pull}} = K(z_0 + v \times t) - Kz_{\text{com}} \quad (1)$$

where F_{pull} represents the external force applied to hydrogen atoms; K is the spring stiffness coefficient and is constant, with a value of 0.01 kcal mol^{-1} nm^{-2} in this study. z_0 is the initial centroid position of the hydrogen atom subjected to external force in the z direction; v is the velocity of the external force applied to the hydrogen atom, set to 0.0025 nm ps^{-1} in this study. t stands for the simulation time, z_{com} is the centroid position of hydrogen atom in the z direction. The entire pull-out simulation lasted 2000 ps. The formula for calculating the interfacial interaction energy between epoxy resin and functionalized carbon nanotubes is as follows:

$$E = E_{\text{total}} - E_{\text{epoxy}} - E_{\text{cnts}} \quad (2)$$

where ΔE represents the energy of composites; E_{total} stands for the energy of the whole system; E_{epoxy} and E_{cnts} are the energy of epoxy and CNTs respectively.

3 Results and discussion

3.1 Influence of functionalized-CNTs on the microstructures of epoxy resin

3.1.1 Atomic distribution of epoxy resin. In this subsection, the influence of functional groups on the atomic distribution of epoxy resin around CNTs in the crosslinking process is described by calculating the radial density distribution. The left view of the CNTs/epoxy resin composite is depicted in Fig. 2. The influence of functional groups on the atomic density distribution is investigated, with CNTs serving as the center and the carbon atoms of CNTs as the initial reference point, using radius r. The analysis is performed on a system with a final crosslinking degree of 86% in order to minimize the impact of varying crosslinking degrees on the atomic density distribution. The area of interest is indicated by the blue shadowed region. An atomic oxygen representative of epoxy resin is selected for study. Fig. 3 presents the radial density distribution of oxygen atoms in epoxy resin under the influence of different functionalized CNTs. It is observed that the oxygen atom density near the CNTs is highest in the CNT-COOH system, and lowest in the CNT system, which aligns with the polarity of the functional groups, demonstrating that epoxy molecules in the CNT-

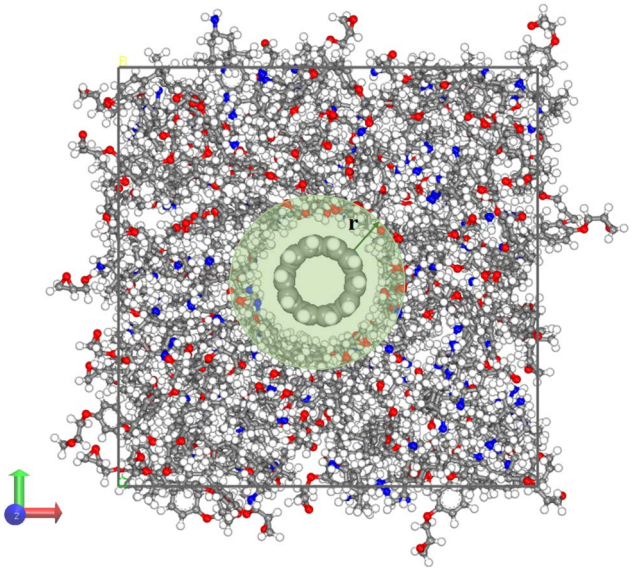

Fig. 2 Left view of CNTs/epoxy system.

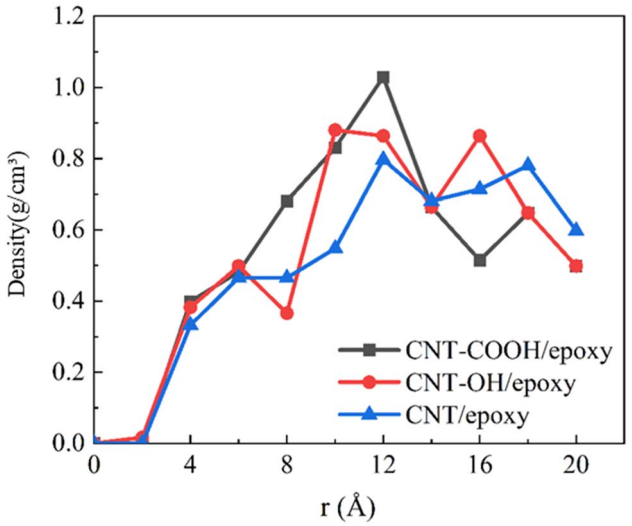

Fig. 3 Radial density distribution of oxygen in epoxy resin.

COOH system exhibit better aggregation near the CNTs. Most of the oxygen atoms are distributed near 10 Å with density peaks of 1.02 g cm^{-3}, 0.88 g cm^{-3}, and 0.78 g cm^{-3}, respectively, indicating that functionalized CNTs can enhance the distribution of epoxy resin near the interface. In the CNT/epoxy system, the oxygen atoms in the epoxy resin are evenly distributed near the interface. However, the functionalization of CNTs leads to significant changes in the distribution of the epoxy resin, making the peak value of the epoxy resin near 10 Å more pronounced. The impact of functionalization is particularly noticeable in the region of 6–14 Å, where the oxygen atom density distribution exhibits a distinct difference.

3.1.2 Interfacial crosslinking degree. In this subsection, the impact of functionalization on the degree of interfacial crosslinking will be evaluated. It has been demonstrated in previous sections that functionalization can enhance the distribution of epoxy resin around CNTs. However, the question remains as to how functionalization of CNTs affects the cross-linking degree at the interface with epoxy resin, and the influence of epoxy resin with the same crosslinking degree on different functionalized CNTs. A thorough analysis will be conducted to address these questions. Fig. 2 illustrates the left view of the CNT-OH/epoxy composite. In this representation, a range of 5 Å centered on CNTs is considered to represent the extent of epoxy crosslinking affected by functionalized CNTs. Fig. 4 displays the degree of crosslinking in the vicinity of the interface of epoxy resins, under the influence of different functionalized CNTs, with different crosslinking degrees. When epoxy resin undergoes cross-linking, CNTs occupy the center of the epoxy resin, and its functionalization will also impact the crosslinking of the epoxy resin. Here, several representative crosslinking degrees are selected, including composites with crosslinking degrees of 20%, 40%, 60%, and 86%. As indicated in Fig. 4, CNTs with different functionalization have only a minimal effect on the crosslinking of epoxy resin at the interface, with the improvement effect of functionalization being negligible. However, with increasing crosslinking degree of the composite, the effect of functionalization becomes increasingly pronounced. The presence of functional groups significantly enhances the crosslinking degree of epoxy resin near the interface, with the crosslinking degree of CNT-COOH/epoxy composite being higher than that of CNT-OH/epoxy.

3.1.3 Fractional free volume. According to the free volume theory, proposed by Fox and Flory[44] in 1949, the volume of solid or liquid materials is divided into occupied and free volume. The free volume, being the unoccupied part of the system, is related to the composition, structure, and packing of the system. Analysis of free volume can provide a deeper understanding of intermolecular accumulation and the spatial state of polymers. Calculation of free volume is conducted using the Monte Carlo algorithm, which involves randomly inserting

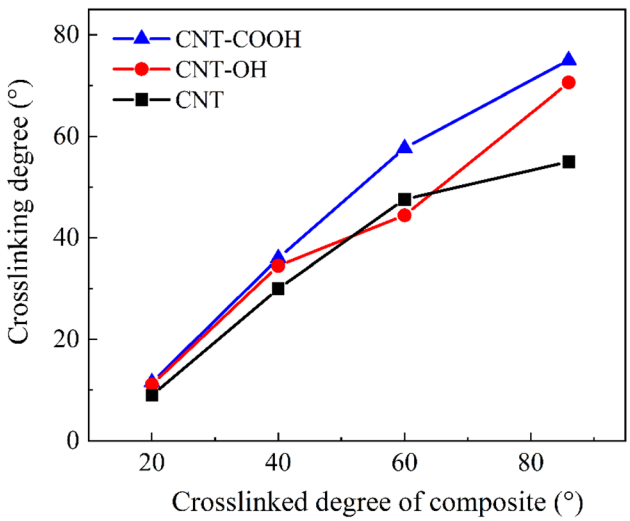

Fig. 4 Effect of functionalization on crosslinking degree of epoxy/carbon nanotube interface.

a probe ball with a specified radius into the system. In this research, the probe radius is 1.4 Å. The probe atoms move within the system and interact with the system atoms to form a contact surface. The region surrounded by the contact surface represents the occupied volume of the system atoms, while the unoccupied region represents the free volume. The volume of the system is defined as V, the occupied volume as V_0, the free volume as V_f, and the fractional free volume (FFV) is introduced.

$$\mathrm{FFV} = \frac{V_f}{V_0 + V_f} \times 100\% \quad (3)$$

The values of V_0, V_f, and FFV for various systems are computed and presented in Table 1. These values are employed to analyze the impact of functionalization on the fractional free volume of the system. As shown in Fig. 5(a), the free volume diagram of the CNT-OH/epoxy resin system with a 86% cross-linking degree at 300 K is depicted. The gray and blue areas represent the free volume surface area and free volume, respectively.

The FFV of various functionalized epoxy resin systems are determined. As seen in Fig. 5(b), the FFV exhibits a decreasing trend with the incorporation of functional groups on the CNTs. Upon the addition of functional groups on the CNTs, a significant decrease in the FFV is observed, and the greatest reduction is noted in the CNT-COOH system. This trend indicates that functionalization leads to a denser accumulation of polymer in the system, suggesting that functionalization will increase the intermolecular interaction between CNTs and epoxy resin. This could also account for the effect of partial functionalization, as discussed in 3.1.1, on the density distribution of epoxy resin. Given that functionalization results in a decrease in the FFV and a more compact arrangement of the system, the density distribution of epoxy resin near the interface is observed to follow the order: CNT-COOH > CNT-OH > CNT.

3.2 Enhancing mechanism of functionalized-CNTs on the interfacial bonding properties

3.2.1 De-bonding behaviors of CNT/epoxy interface. In this subsection, the impact of functionalization on interfacial adhesion is analyzed using force–displacement curves derived from the pull-out process. The examination of functionalized CNTs to enhance interfacial bonding performance will be explored in the subsequent section.

The pull-out process of CNTs can be described as follows: firstly, an initial configuration is optimized through geometric optimization and dynamic relaxation to attain an acceptable equilibrium configuration. Fixing a portion of the epoxy is crucial in preventing the rigid motion of the epoxy resin. Secondly, an external force is applied to a subset of CNT atoms. The formula for calculating external force is listed in 2.2. Finally, the structure with the lowest energy is obtained through relaxation. After repeated loading, the CNTs are completely detached from the epoxy resin. The representative snapshot in Fig. 6 displays the dynamic pull-out simulation, which is employed to investigate the interfacial bonding performance. At 0 ps, a dynamic equilibrium between the CNTs and epoxy resin is established. Furthermore, at this simulation time, the pull-out distance of CNTs in the CNT-COOH/epoxy system is the smallest among all systems, which, in conjunction with the observation that a small amount of epoxy resin remains adhered to the CNTs after full detachment, suggests the existence of robust interfacial adhesion between the CNTs and epoxy resin in the CNT-COOH/epoxy system. Additionally, it is noted that most epoxy resins adhere to functional groups, suggesting that functionalization can improve the interfacial adhesion between epoxy resin and CNTs.

Fig. 7(a) depicts the force–displacement relationship of various CNTs during the pull-out simulation. The load–displacement curve displays a periodic multi-peak phenomenon, which is strongly related to the breaking and reforming of the interface chemical bonds. The maximum shearing force that the CNTs can sustain is also closely correlated with the interface interaction. The maximum pulling force applied to the CNTs can be extracted from the force–displacement curve, as shown in Fig. 7(b). The maximum external force applied to the CNTs in the CNT-COOH/epoxy system is 5.25×10^{-9} N, while the maximum force applied in the CNT-OH/epoxy system is 4.49×10^{-9} N. In contrast, only 1.344×10^{-9} N is applied to the CNT/epoxy system, which is the lowest and coincides with the polarity of the functional groups. The results indicate that functionalization enhances the interfacial adhesion between the CNTs and epoxy resin. To further investigate this effect, the work of pulling force applied on the CNTs during the simulation was calculated, as shown in Fig. 8(a). The work done by the pulling force follows the sequence: CNT-COOH/epoxy > CNT-OH/epoxy > CNT/epoxy, which is consistent with the magnitude of the pulling force. This suggests that functionalization constitutes an effective approach to improve the interfacial adhesion between epoxy resin and CNTs. The microscopic mechanism underlying this improvement in mechanical properties will be explored in the subsequent section.

Fig. 8(b) presents the interaction energy between epoxy resin and carbon nanotubes in various systems at an equilibrium stage. The interaction energy between the CNTs and epoxy resin is estimated to be approximately -475 kcal mol^{-1} in the absence of functionalization. The CNT-OH/epoxy system exhibits an interaction energy of -552 kcal mol^{-1}, representing an increase of approximately 16.2%. In the CNT-COOH/epoxy system, the interaction energy is further increased by approximately 20%. The functionalization of CNTs leads to varying degrees of increased interaction energy between the epoxy resin and CNTs, suggesting that functionalized CNTs can enhance the interaction between the two materials. This observation

Table 1 The calculated V_o, V_f and FFVs of different functionalized CNT/epoxy system

Systems	CNT/epoxy	CNT-OH/epoxy	CNT-COOH/epoxy
Occupied volume (Å^3)	69774.58	71615.99	72085.25
Free volume (Å^3)	10225.42	8384.01	7914.75
FFV (%)	12.78%	10.48%	9.89%

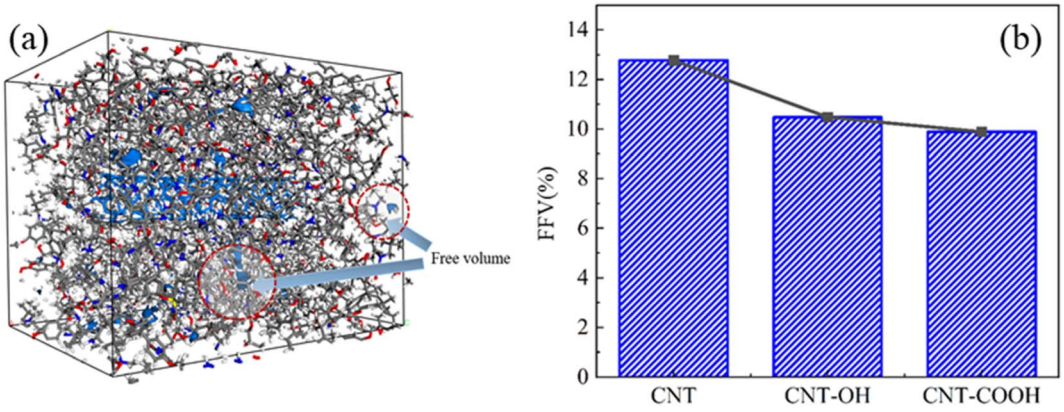

Fig. 5 (a) The free volume diagram of CNT-OH/epoxy resin system with 86% crosslinking degree; (b) the FFV of different functionalized epoxy resin systems.

helps explain why CNTs exhibit varying levels of adhesion to the epoxy resin when completely extracted from the resin. High interaction energy confers a strong adhesive property at the composite interface, and constitutes compelling evidence for the enhanced mechanical properties of CNT-reinforced epoxy resin.

3.2.2 Interfacial reinforcement of chemical bonds. The alteration of pullout force and interface bond strength is primarily attributed to variations in interface interaction and load transfer mechanism. The transfer of load is primarily facilitated by interfacial chemical bonds, making the investigation of their mechanism crucial for a comprehensive understanding of how functionalization improves mechanical performance.

The enhancement of interfacial strength between functionalized CNTs and epoxy resin is closely tied to the chemical bonds present at the interface. This section explains the reason behind the difference in force–displacement curves by analyzing the changes in ionic and hydrogen bonds at the interface of functionalized CNTs. These chemical bonds are analyzed qualitatively using radial distribution functions (RDFs), which serve to reflect the spatial relationships between atoms. For the sake of simplicity, hydroxyl hydrogen (ho_{CNT}), hydroxyl oxygen (ho_{CNT}), and double bond oxygen (ho_{CNT}) represent the atoms of CNTs, while hydroxyl hydrogen (ho_{epoxy}), hydroxyl oxygen (oh_{epoxy}) and nitrogen atoms (N_{epoxy}) represent the atoms of epoxy resin. As shown in Fig. 9, for the CNT/epoxy composite, the RDF of C_{CNT}–N_{epoxy}, C_{CNT}–Oh_{epoxy} and H_{CNT}–O_{epoxy} did not display a clear peak, indicating that ion pairs and hydrogen bonds cannot form between epoxy resin and CNTs, which is consistent with the findings of Zhang *et al.*[45] This inability to form chemical bonds at the interface leads to low

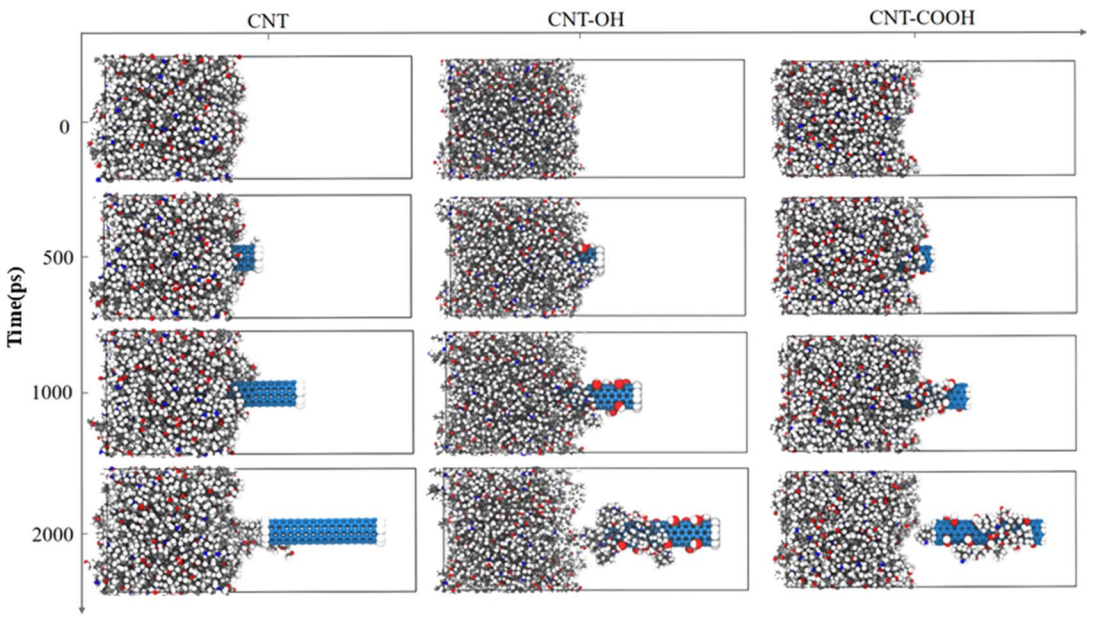

Fig. 6 Snapshots of the pull-out process of CNTs at 0 ps, 500 ps, 1000 ps and 2000 ps.

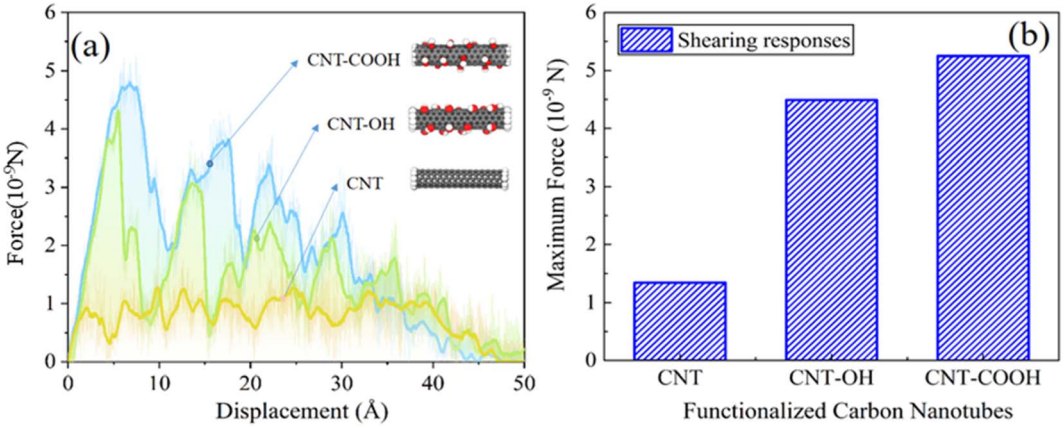

Fig. 7 (a) The load–displacement of various systems. (b) The maximum pulling force applied to the carbon nanotubes.

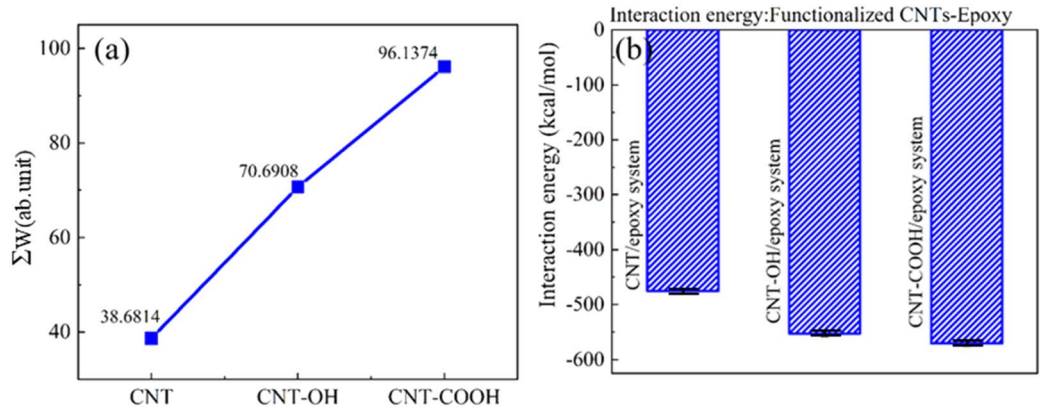

Fig. 8 (a) The work done by pulling force. (b) The interaction energy between functionalized CNT-epoxy.

interfacial bond strength, which is in agreement with the conclusions drawn from previous pull-out simulations. Given the absence of chemical bonds at the interface of CNT-epoxy composites, the following section will not delve further into this topic.

For CNT-OH/epoxy composite, the RDF between N_{epoxy} and ho_{CNT} displays the obvious peaks at 2.05 Å, indicating that ions pairs can be developed between epoxy resins and CNTs. And the same ion pair is formed in CNT-COOH/epoxy composite, indicating that ion pairs can be formed at the interface of the two systems, as dispicted in Fig. 10(a). However, the intensity of the RDF peak (N_{epoxy}–ho_{CNT}) in CNT-OH/epoxy composite is lower than that of the counterpart in CNT-COOH/epoxy composite. The low strength of RDF peak indicates that the attraction between N_{epoxy} atom (epoxy) and ho_{CNT} atom (CNT) in CNT-OH/epoxy composites is weak. As shown in Fig. 10(b), this trend can be quantified by the average coordination number of N_{epoxy}–ho_{CNT} pairs. By comparing the configuration snapshots of the interface region (Fig. 10(c) and (d)) in CNT-COOH/epoxy composite and CNT-OH/epoxy composite, the epoxy resin is attracted to the CNTs, which contributes to the improvement of interfacial bonding performance. At the same time, it also explains from the perspective of bonding that CNTs COOH and

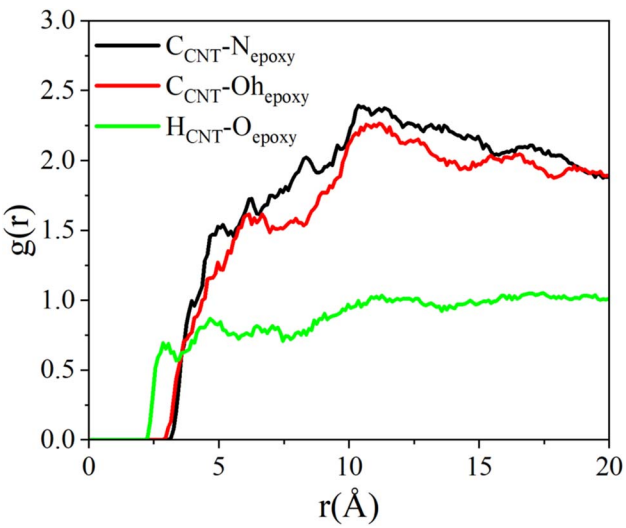

Fig. 9 RDFs between carbon atoms on carbon nanotubes and nitrogen atoms on epoxy resins; carbon atoms on carbon nanotubes and hydroxyl oxygen atoms on epoxy resins; hydrogen atoms on the carbon nanotubes and oxygen atoms on the epoxy resin in CNT/epoxy system.

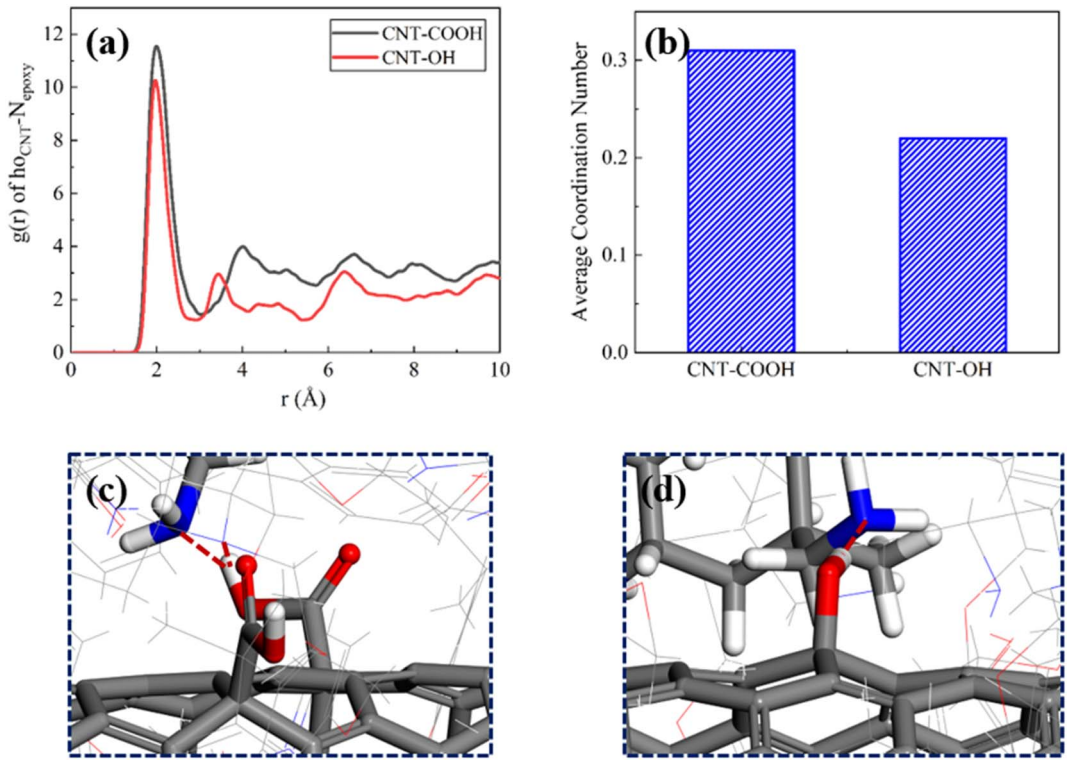

Fig. 10 (a) RDFs between hydroxyl hydrogen atoms on carbon nanotubes and nitrogen atoms on epoxy resins; (b) the average coordination number; (c) snapshots of H–N pair in CNT-COOH/epoxy composite; (d) H–N pair in CNT-OH/epoxy composite.

epoxy resin matrix have formed better interfacial bonding performance and shear strength in other works.[46]

The RDF between Nepoxy and ho$_{CNT}$ in the CNT-OH/epoxy composite reveals clear peaks at 2.05 Å, demonstrating the presence of ion pairs between the epoxy resin and carbon nanotubes (CNTs). A similar ion pair is observed in the CNT-COOH/epoxy composite, implying that ion pairs can be formed at the interface between the two systems, as depicted in Fig. 10(a). However, the intensity of the RDF peak (N$_{epoxy}$–ho$_{CNT}$) in the CNT-OH/epoxy composite is lower than that in the CNT-COOH/epoxy composite. This low intensity suggests a weak attraction between the N$_{epoxy}$ (epoxy) and ho$_{CNT}$ atoms in the CNT-OH/epoxy composite. As shown in Fig. 10(b), this trend can be quantified by the average coordination number of N$_{epoxy}$–ho$_{CNT}$ pairs. Comparison of the configuration snapshots of the interface region in the CNT-COOH/epoxy composite and CNT-OH/epoxy composite (Fig. 10(c) and (d)) reveals that the epoxy resin is attracted to the CNTs, enhancing interfacial bonding performance.

Besides the H–N bond, the hydrogen bond networks established between epoxy resin and carbon nanotubes are also substantial contributors to the interfacial adhesion properties. Fig. 11 quantifies the hydrogen bond networks between the epoxy resin and CNTs when the epoxy resins act as hydrogen donors and acceptors. As depicted in Fig. 11(a), the hydroxyl hydrogen atom of the epoxy resin and the double bond oxygen atom of the CNTs form a significant peak at 1.85 Å, indicating the formation of hydrogen bonds between the epoxy resin and CNTs. Furthermore, the appearance of the first peak occurs at a position smaller than the hydrogen bond formation threshold, demonstrating the epoxy resin's provision of hydrogen as a hydrogen bond donor to establish a hydrogen bond network with the CNTs. However, the RDF peak of the hydrogen bond in the composite system of carboxyl-functionalized CNTs is higher compared to that of hydroxyl-functionalized CNTs. This trend can be quantified by coordination numbers (CN). The CN of ho$_{epoxy}$–Od$_{CNT}$ in the CNT-COOH/epoxy composite is 0.31, higher than that of the CNT-OH/epoxy composite. This trend is also discernible in Fig. 11(b). As a hydrogen acceptor, the epoxy resin forms hydrogen bonds with the CNTs, and the RDF peak intensity of CNT-COOH is higher than that of CNT-OH, which aligns with the trend indicated in the force-displacement curve. Thus, the incorporation of functional groups not only enhances the formation of ion pairs between the epoxy resin and CNTs but also strengthens the hydrogen bond networks.

The RDF analysis qualitatively captures the functionalization's promotion of interaction between the CNTs and epoxy resin, while the average coordination number quantitatively describes the interaction between the two atomic bonds. The time correlation function (TCF) is utilized to evaluate the dynamic behavior of the atoms. In the following section, the TCF is employed to evaluate the dynamic stability of the ion pairs.

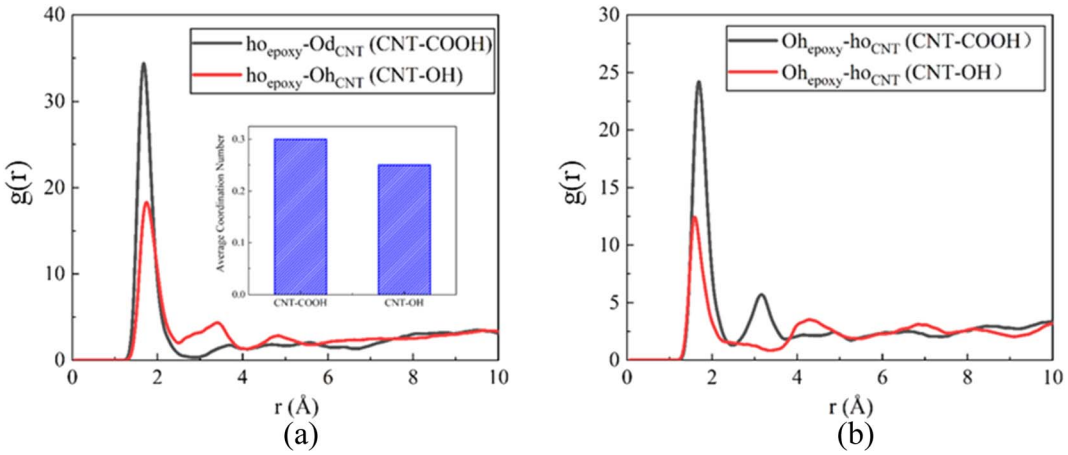

Fig. 11 (a) RDFs between hydroxyl hydrogen atoms on epoxy resins and oxygen atoms on carbon nanotubes; the average coordination number (b) RDFs between hydroxyl oxygen atoms on epoxy resins and hydroxyl hydrogen atoms on carbon nanotubes.

4 Conclusions

In this study, the impact of functionalized CNTs on the interfacial adhesion between epoxy resin and CNTs was investigated. The force–displacement curves were determined, and the bond interaction and dynamic properties of the functionalized CNTs-epoxy resin system were evaluated. This molecular dynamics analysis provides insight into the reinforcement of epoxy resin by nanomaterials. The conclusions can be summarized as follows:

1. Functionalization enhances the density distribution and crosslinking degree of the epoxy resin at the interface. The improvement effect of functionalization increases with an increase in the crosslinking degree of the composite. Additionally, functionalization reduces the free volume fraction and increases the density of the composite.

2. Simulation of pull-out tests reveals that functionalization enhances the bonding between the epoxy resin and CNTs. The peak value of external force in the CNT-COOH/epoxy resin system was slightly higher than in the CNT-OH/epoxy resin system, indicating that carboxyl functionalized CNTs have improved bonding properties. Complete stripping of the epoxy resin revealed that functionalized CNTs can adhere to some epoxy resin, providing evidence of improved bonding performance.

3. Micro analysis highlights the reasons for the improved interfacial adhesion. The strong interaction between the epoxy resin and CNTs is the primary factor contributing to the good bonding performance of the composite. Additionally, functional CNTs form hydrogen bond networks with the epoxy resin. The polar functional groups on the CNTs attract more epoxy resin to the interface, thereby improving the interfacial bonding performance. Analysis of the bonding stability revealed that the strong stability of hydrogen bonds and ionic bonds contributes to the high interfacial bonding performance.

Conflicts of interest

There are no conflicts of interest to declare.

Acknowledgements

Financial support from National Natural science foundation of China under Grant U2006224, 52178221, 51978352, 51908308, Natural science foundation of Shandong Province under Grant ZR2020JQ25, ZR2022YQ55, 2019KJG010, Taishan Scholars of Shandong Province under Grant tsqn.201812090, are gratefully acknowledged.

References

1 W. Liu, Y. Wang, P. Wang, Y. Li, Q. Jiang, X. Hu, Y. Wei, Y. Qiu, S. I. S. Shahabadi and X. Lu, *Composites, Part B*, 2017, **113**, 197–205.
2 S.-C. Shiu and J.-L. Tsai, *Composites, Part B*, 2014, **56**, 691–697.
3 A. Kumar, P. K. Ghosh, K. L. Yadav and K. Kumar, *Composites, Part B*, 2017, **113**, 291–299.
4 A. J. Kinloch, S. H. Lee and A. C. Taylor, *Polymer*, 2014, **55**, 6325–6334.
5 N. Parhizkar, B. Ramezanzadeh and T. Shahrabi, *Appl. Surf. Sci.*, 2018, **439**, 45–59.
6 Z. Zheng, Y. Li, S. A. He, X. Ma, X. Zhu and S. Li, *Constr. Build. Mater.*, 2019, **197**, 319–330.
7 S.-Y. Guo, X. Zhang, J.-Z. Chen, B. Mou, H.-S. Shang, P. Wang, L. Zhang and J. Ren, *Constr. Build. Mater.*, 2020, **264**, 319–330.
8 S.-Y. Guo, X. Zhang, J. Ren, J.-Z. Chen, T.-J. Zhao, T.-W. Li and L. Zhang, *Constr. Build. Mater.*, 2021, **272**, 960.
9 A. Dadrasi, G. A. Farzi, M. Shariati, S. Fooladpanjeh and V. Parvaneh, *Eng. Fract. Mech.*, 2020, **232**.
10 P. S. Yadav, R. Purohit and A. Kothari, *Mater. Today: Proc.*, 2019, **18**, 5530–5539.
11 P. Ma, G. Jiang, Q. Chen, H. Cong and X. Nie, *Composites, Part B*, 2015, **69**, 526–533.
12 S. A. Bansal, V. Khanna, A. P. Singh and S. Kumar, *Mater. Today: Proc.*, 2021, 275–279.
13 J. Goclon, T. Panczyk and K. Winkler, *Appl. Surf. Sci.*, 2018, **433**, 213–221.

14 S. Iijima, *Nature*, 1991, **354**, 56–58.
15 B. Hao, Q. Ma, S. Yang, E. Mäder and P.-C. Ma, *Compos. Sci. Technol.*, 2016, **129**, 38–45.
16 Y. Li, S. Wang, Q. Wang and M. Xing, *Composites, Part B*, 2018, **133**, 35–41.
17 H. Khoramishad and M. Khakzad, *J. Adhes.*, 2016, **94**, 15–29.
18 S. Yu, M. N. Tong and G. Critchlow, *Mater. Des.*, 2010, **31**, S126–S129.
19 S. Aodkeng, S. Sinthupinyo, B. Chamnankid, W. Hanpongpun and A. Chaipanich, *Constr. Build. Mater.*, 2022, **320**, 212.
20 W.-M. Qian, M. H. Vahid, Y.-L. Sun, A. Heidari, R. Barbaz-Isfahani, S. Saber-Samandari, A. Khandan and D. Toghraie, *J. Mater. Res. Technol.*, 2021, **12**, 1931–1945.
21 J. Patil, H. Patil, R. Sankpal, D. Rathod, K. Patil, P. R. Kubade and H. B. Kulkarni, *Mater. Today: Proc.*, 2021, **46**, 7182–7186.
22 X. Chen, F. Peng, C. Wang, H. Zhou, X. Lin, W. Liu and A. Zhang, *Appl. Surf. Sci.*, 2022, **576**, 765.
23 B. Suresha, N. M. Indushekhara, C. A. Varun, D. Sachin and K. Pranao, *Mater. Today: Proc.*, 2021, **43**, 1478–1484.
24 D. Hou, Q. Yang, Z. Jin, P. Wang, M. Wang, X. Wang and Y. Zhang, *Appl. Surf. Sci.*, 2021, **568**, 896.
25 J.-H. Sul, B. Gangadhara Prusty and D. W. Kelly, *Adv. Manuf.: Polym. Compos. Sci.*, 2015, **1**, 94–104.
26 C. Baudot and C. M. Tan, *Int. J. Nanotechnol.*, 2009, **6**, 618–627.
27 D. S. Hou, Q. R. Yang, Z. Q. Jin, P. Wang, M. H. Wang, X. P. Wang and Y. Zhang, *Appl. Surf. Sci.*, 2021, **568**, 11.
28 P. Wang, Q. R. Yang, Z. Q. Jin, D. S. Hou and M. H. Wang, *J. Mater. Sci.*, 2021, **56**, 16475–16490.
29 Z. Q. Mao, W. Wu, Y. Cheng, C. Xie, D. M. Zhang and X. Q. Jiang, *J. Nanosci. Nanotechnol.*, 2011, **11**, 5169–5178.
30 Z. Abousalman-Rezvani, P. Eskandari, H. Roghani-Mamaqani and M. Salami-Kalajahi, *Adv. Colloid Interface Sci.*, 2020, **278**, 102126.
31 M. Liebscher, T. Gärtner, L. Tzounis, M. Mičušík, P. Pötschke, M. Stamm, G. Heinrich and B. Voit, *Compos. Sci. Technol.*, 2014, **101**, 133–138.
32 N. T. Dintcheva, R. Arrigo, E. Morici, C. Gambarotti, S. Carroccio, F. Cicogna and G. Filippone, *Composites, Part B*, 2015, **82**, 196–204.
33 N. G. Sahoo, S. Rana, J. W. Cho, L. Li and S. H. Chan, *Prog. Polym. Sci.*, 2010, **35**, 837–867.
34 L. Wang, Y. Tan, X. Wang, T. Xu, C. Xiao and Z. Qi, *Chem. Phys. Lett.*, 2018, **706**, 31–39.
35 P.-C. Ma, S.-Y. Mo, B.-Z. Tang and J.-K. Kim, *Carbon*, 2010, **48**, 1824–1834.
36 H. Jung, H. K. Choi, S. Kim, H.-S. Lee, Y. Kim and J. Yu, *Composites, Part A*, 2017, **103**, 17–24.
37 C. Hirschl, M. Biebl-Rydlo, M. DeBiasio, W. Mühleisen, L. Neumaier, W. Scherf, G. Oreski, G. Eder, B. Chernev, W. Schwab and M. Kraft, *Sol. Energy Mater. Sol. Cells*, 2013, **116**, 203–218.
38 L. H. Tam and D. Lau, *RSC Adv.*, 2014, **4**, 33074–33081.
39 W.-Y. Chen, Y.-Z. Wang, S.-W. Kuo, C.-F. Huang, P.-H. Tung and F.-C. Chang, *Polymer*, 2004, **45**, 6897–6908.
40 Y. L. Yaphary, Z. Yu, R. H. W. Lam, D. Hui and D. Lau, *Composites, Part B*, 2017, **131**, 165–172.
41 O. Buyukozturk, M. J. Buehler, D. Lau and C. Tuakta, *Int. J. Solids Struct.*, 2011, **48**, 2131–2140.
42 F. Sanchez and L. Zhang, *Carbon*, 2010, **48**, 1210–1223.
43 S. Plimpton, P. Crozier and A. Thompson, *Sandia Natl. Lab.*, 2007, **18**, 43.
44 T. G. Fox and P. J. Flory, *J. Appl. Phys.*, 1950, **21**, 581–591.
45 W. Q. Zhang, Y. Qing, W. H. Zhong, G. Sui and X. P. Yang, *React. Funct. Polym.*, 2017, **111**, 60–67.
46 W. Zhang, X. Deng, G. Sui and X. Yang, *Carbon*, 2019, **145**, 629–639.